https://doi.org/10.26682/sjuod.2023.26.2.40
Journal of University of Duhok., Vol. 26, No.2 (Pure Engineering Sciences),Pp 466-479, 2023

THE ELECTRONIC STRUCTURE, STABILITY, THERMODYNAMICS AND VIBRATIONAL STUDY OF CIS ALKENYL SUBSTITUTED CHALCONES BY DENSITY FUNCTIONAL THEORY CALCULATIONS

HAVAL **A**.**H**USSEIN
Dept. of Chemistry, College of Science, University of Duhok, Kurdistan Region-Iraq

(Received: October 15, 2023; Accepted for Publication: December 24, 2023)

ABSTRACT

In this research, structural analysis and stability of six *cis* chalcone conformers were investigated, compared with *trans* conformers using the DFT-B3LYP method and basis set 6-311++G(d,p). Results obtained found that 1-Butenyl *cis* Chalcone (1-BC) possesses the greatest stability. The polarity of the solvent and the geometry of the conformer appeared to have a significant impact on the stability of the conformers. Additionally, *cis* 1-BC was appeared to cause the greatest shifts (7 cm^{-1}-gas,6 cm^{-1}-n-hexane and 6 cm^{-1}-ethanol) in the magnitudes of vibrational frequencies of *cis* unsubstituted CA followed by *cis* divinyl chalcone (DVC) and *cis* *E*-propenyl chalcone (*E*-PC). It is revealed that the 2-butenyl chalcone (2-BC) constitutes the highest values of Thermal-Energy (T-E), Entropy- (S) and Heat -Capacity (C_v).

***KEYWORDS*:** Stability, *cis* chalcone, DFT, FMO, MEP and NLO.

1. INTRODUCTION

Chalcones are dyes that are naturally exist in edible plants and commonly found in natural products such as vegetables, fruits, and other food products [Carlo *et al.*, 1999; Zaini *et al.*, 2019]. Chalcones belong to the flavonoid's family, a class of naturally occurring synthetic organic compounds commonly known as benzylideneacetophenones [Kostanecki and Tambor,1899]. They are intermediates that enter the synthesis of flavonoids and isoflavonoids [Abbas *et al.*, 2014]. Chalcone derivatives are vital to producing many heterocyclic compounds as they have known outstanding nonlinear optical (NLO) characteristics [Zaini *et al.*, 2019; Goto *et al.*, 1991]. Natural and synthetic derivatives of chalcones have a variety of interesting pharmacological applications have been proposed for natural and synthetic chalcones, including biological [Broichhagen *et al.*, 2015], antifungal [Venkata *et al.*, 2017], anti-inflammatory [Ibrahim *et al.*, 2021], antileishmanial [Escrivani *et al.*, 2021], antimalarial [Qin *et al.*,2020], analgesic [Lakshminarayanan *et al.*, 2020], antibacterial[Okolo *et al.*, 2021], and antidiabetic[Kahssay *et al.* ,2021] uses, as well as aldose reductase[Reddy *et al.*, 2019] and non-purine xanthine oxidase inhibition[Bui *et al.*, 2016], depending on the substitution patterns on the phenyl rings in chalcones. Chalcones display a vital action in biology due to their anti-oxidant and anti-cancer properties[Zhuang *et al.*, 2017].Recently, chalcone derivatives have shown potential applications in photonic devices, for example, in optical switching, erasable memory media, and optical data storage systems, as they are photochromic materials that display a solid-state appearance or fluorescence colour changes if exposed to light [Xie *et al.*, 2021].

Hussein and Fadhil (2020) investigated the structure and stability of dichloro amino derivatives of chalcones and found that the more conjugated and planar closed chromene isomers were the most stable. The *cis* isomers of chalcones were the least stable due to steric hindrance. Naresh *et al.* (2021) investigated and characterised the structural and electronic properties of two new geometrical isomers of thiophene chalcones derivatives. They found that the *E*-isomer was more stable and that the electronic properties of these molecules were highly reliable in terms of the π-conjugation framework.

The previous study [Hussein,2023] focused on the stability of *trans* alkenyl substituted conformers of chalcones and the results shown that *trans* conformers apparently possessed highest magnitudes of stability as the result of greater planarity existing in their conformers. Additionally, different magnitudes of thermodynamic parameters were noted in *trans*

conformers and they also found to follow a different protocol as compared with *cis* conformers.

The current study aimed to analyse the structure and stability of six *cis* conformers of chalcones with varied lengths of aliphatic alkenyl substituents (table 1) using DFT approach and B3LYP functional. The thermodynamic parameters involving the enthalpy of hydrogenation (ΔH), thermal energy (*TE*) entropy (*S*) and heat capacity at constant volume (C_v) were found and vibrational frequencies for carbonyl group were also analysed. Finally, to understand the effect of solvent, the above parameters were calculated in polar (ethanol) and nonpolar (n-hexane) media.

Table (1): *Cis* conformers of chalcones.

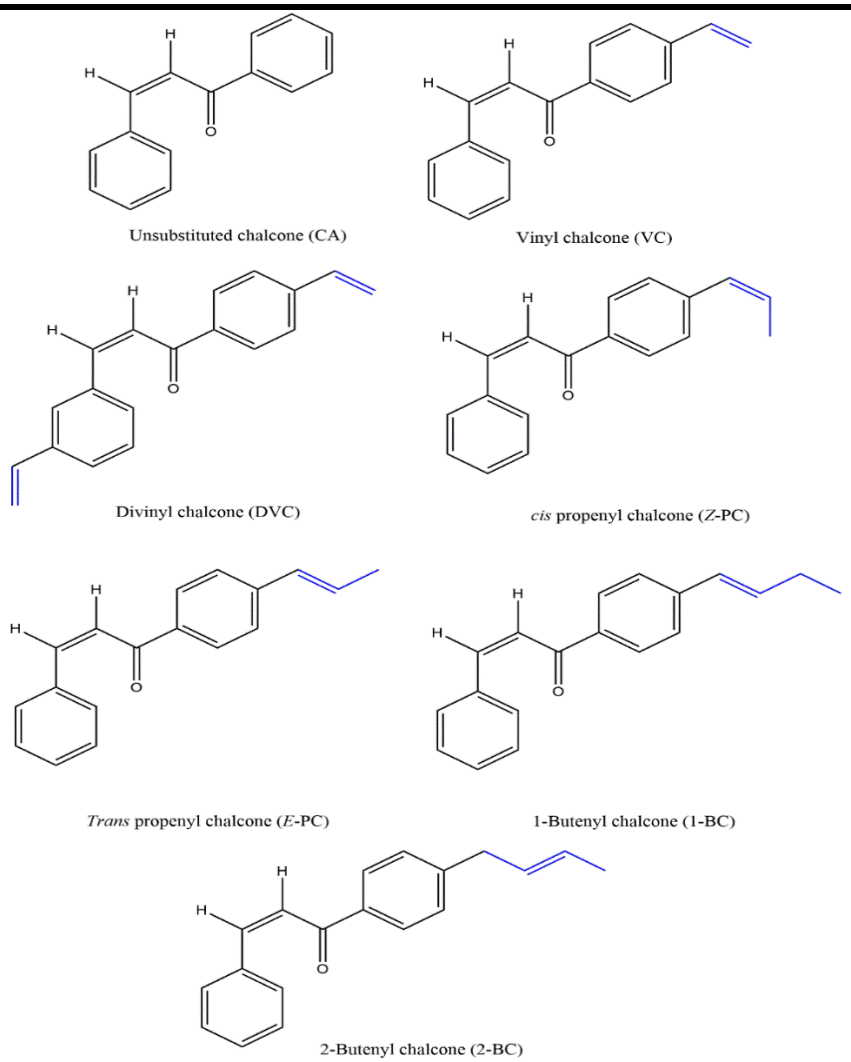

2.METHODS OF CALCULATIONS

The Gaussian version 09 [Frisch *et al.*, 2013] and the Gauss view 5.0 software [Dennington *et al.*, 2009] were utilized to perform computations and geometry optimization for the ground state conformers. The ground state conformers of *cis* chalcones were geometry optimized using density functional theory (DFT) [Stephens *et al.*, 1994] as a method, B3LYP [Becke, 1993; Lee *et al.*,1988] as a functional standing for the Becke 3 parameter Lee Yang Parr and 6-311 ++ G(d,p) basis set. We estimated the solvent impact by the PCM (Polarizable Continuum Model) solvation model [Tomasi *et al.*, 1999; Tomasi *et al.*, 2005;Mohbiya and Sekar, 2018]. The true minimum or a stationary point for the optimized structures was affirmed by measuring the vibrational frequencies for the asymmetric C=O stretching and ensuring the absence of imaginary frequency. We scaled the vibrations by 0.983 and by 0.958 for frequencies less and higher than

1700 cm^{-1},respectively in the gas phase, n-hexane, and ethanol [Balci and Akyuz, 2008;Sundaraganesan *et al.*, 2005].

3.RESULTS AND DISCUSSION

The stability and structural analysis of six conformers of *cis* chalcone with varied substituents (Table 1) appeared to be influenced by the extent of π-conjugation and solvent polarity. In this research, the analysis and the results were discussed in separate sections.

3.1 Stability of chalcone

The results in table 2 demonstrate that the value of the total energies and dipole moments for the unsubstituted *cis* chalcone (CA) are different when replacing the hydrogen at the para position with alkenyl groups.

Since the largest π-conjugations owned by *cis* 1-butenyl chalcone (1-BC) that enhances electron delocalisation in this molecule, it tends to significantly decrease the magnitude of the total energy of *cis* 1-BC by 1.56 x 10^2 Hartree, as compared with *cis* CA in the gas phase. Consequently, it substantially improves the stability of *cis* 1-BC.

The findings illustrated that a slightly lower impact is observed when substituting the CA with divinyl chalcone compared with 1-BC, which caused a slightly lower increase in the magnitude of *E* (by 1.55 x 10^2 Hartree-gas phase). For *E*- and *Z*-propenyl substituents, the results revealed a much lower growth in the stability of *cis* CA (by 1.17 x 10^2 Hartree) relative to both divinyl chalcone (DVC) and 1-BC by 38.25 Hartree. The stability of *cis* CA was risen slightly when substituting the *cis* CA with one vinyl group in VC, which increased the stability of *cis* CA by77.29 Hartree gas phase.

The conformer's geometry also influences CA's stability since *trans* CA appeared to possess more stability than *cis* CA by 8.54 x 10^{-3} Hartree. *Trans* CA has higher planarity and hence constitutes higher π-conjugation and electron delocalisation than *cis* CA, which suffers steric hindrance. Additionally, the same stability trend is observed with a slightly lower difference in energy of 8.43 x 10^{-3} Hartree when comparing the rest of the *trans* and *cis* alkenyl substituted conformers. Therefore, alkenyl substituents appeared to follow the same protocol in raising CA stability. Moreover, Table 2 demonstrated that *trans* conformers generally possess higher dipole moments in Debye than the *cis* conformers due to their higher planarity and π-conjugation. Furthermore, the divinyl and 1-butenyl substituents produced the highest increase in the dipole moment of CA by 1 Debye.

Table (2): Total Energy (*E*) in Hartree; dipole moment (DM) in Debye for *cis* and *trans* [Hussein, 2023] chalcones computed by DFT(B3LYP) and 6-311++G(d,p) basis set.

		Cis		***Trans***	
Isomer	Phase	*E*	DM	*E*	DM
CA	Gas	-653.962437	2.2475	-653.970785	3.2446
	n-Hexane	-653.965112	2.6001	-653.974144	3.7195
	Ethanol	-653.970409	3.4370	-653.980483	4.7162
VC	Gas	-731.347486	2.2905	-731.355929	3.2266
	n-Hexane	-731.350459	2.5883	-731.359546	3.6997
	Ethanol	-731.366419	4.5619	-731.366419	4.7071
DVC	Gas	-808.733052	2.7056	-808.741195	3.2837
	n-Hexane	-808.736235	2.5257	-808.745079	3.7754
	Ethanol	-808.742609	3.8009	-808.752508	4.8201
E-PC	Gas	-770.647988	2.5161	-770.656424	3.2624
	n-Hexane	-770.651125	4.3089	-770.660197	3.7551
	Ethanol	-770.657252	4.5207	-770.667338	4.7939
Z-PC	Gas	-770.643432	2.7899	-770.651854	3.0656
	n-Hexane	-770.646349	3.1572	-770.655464	3.5283
	Ethanol	-770.652168	3.8333	-770.662290	4.5013
1-BC	Gas	-809.942329	3.4056	-809.950774	3.2781
	n-Hexane	-809.946291	3.8430	-809.955605	3.7684
	Ethanol	-809.953030	3.7797	-809.964667	4.8151
2-BC	Gas	-809.937979	3.1227	-809.946406	3.1587
	n-Hexane	-809.942817	3.4986	-809.951513	3.6788
	Ethanol	-809.949221	4.2074	-809.958741	4.7372

3.2 The solvent effect

The solvent effect is significant in studying the phenomena of stability, as the difference in polarity can induce a pronounced change in the total energies of conformers in a solution [Hussein, 2023].

In this study, an evaluation of the solvent effects on the stability of *cis* conformer and its para-substituted alkenyl derivatives was carried out using the PCM model. Notably, this model does not include the presence of explicit solvent molecules. Consequently, specific interactions involving solute-solvent are not defined, so solvation effects only arise from the electrostatic polarisation of mutual solute-solvent.[Hussein, 2023]

The results demonstrated that the highest stability was achieved in more polar solvent (ethanol) stabilised due to the solvent dielectric constant. The dielectric constant (ε) of a solvent medium indicates the solvents' ability to separate charges in a given molecule [Valverde *et al.*, 2019]. Therefore, the values of total energies are generally lower in ethanol than in n-hexane, which concurs with the polar character of the studied compounds (table 2) and the dipole moment that increases by increasing the solvent polarity. The stabilisation is expected to be caused by the formation of hydrogen bonding [Sobhi *et al.*, 2017] and dipole-dipole interactions [Miar *et al.*, 2021] in ethanol solvents.

The solvent stabilisation gap was estimated by measuring the energy separations between each of gas phase and n-hexane, the gas phase and ethanol, and ethanol and n-hexane, as depicted in Figure 1. The results illustrated that *cis* conformers possessed a similar trend to that previously discovered in *trans* conformers. On the other hand, a very significant shift in two trends of (ethanol to n-hexane) and (ethanol to gas) was observed with *cis* VC conformers. This variation could be attributed to the nature of stabilisation of the *cis* VC conformer in ethanol solvent, which differs from the rest of the molecules.

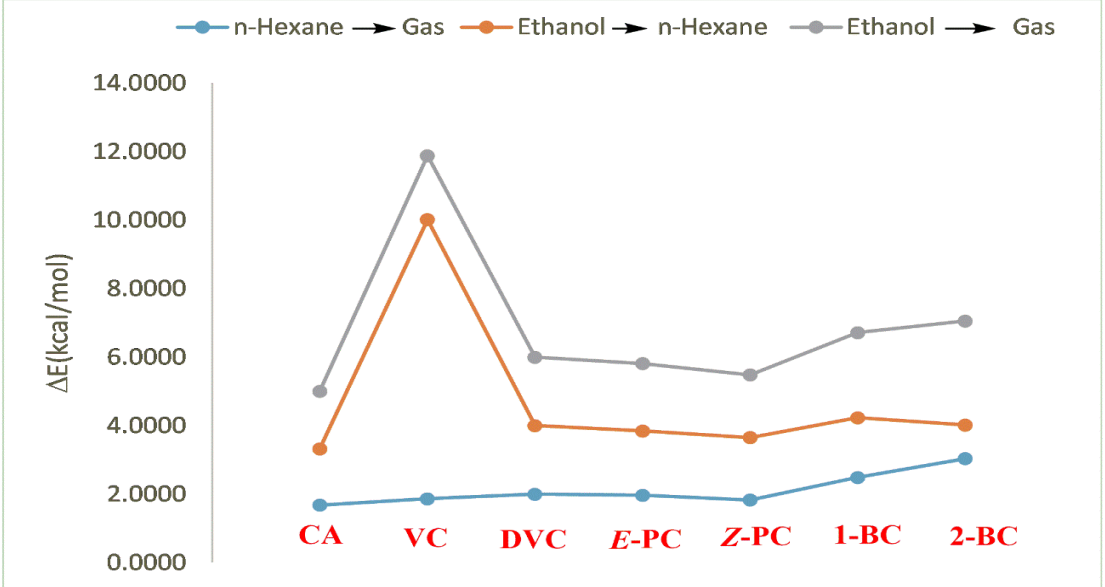

Fig. (1): Energy difference (ΔE) in kcal/mol between ethanol → gas, ethanol → n-hexane and n-hexane → gas. for the *cis* conformers.

In this study, the torsion angles for *cis* conformers represented in Schemes 2 and 3 were evaluated applying DFT/B3LYP//(6-311++G(d,p).

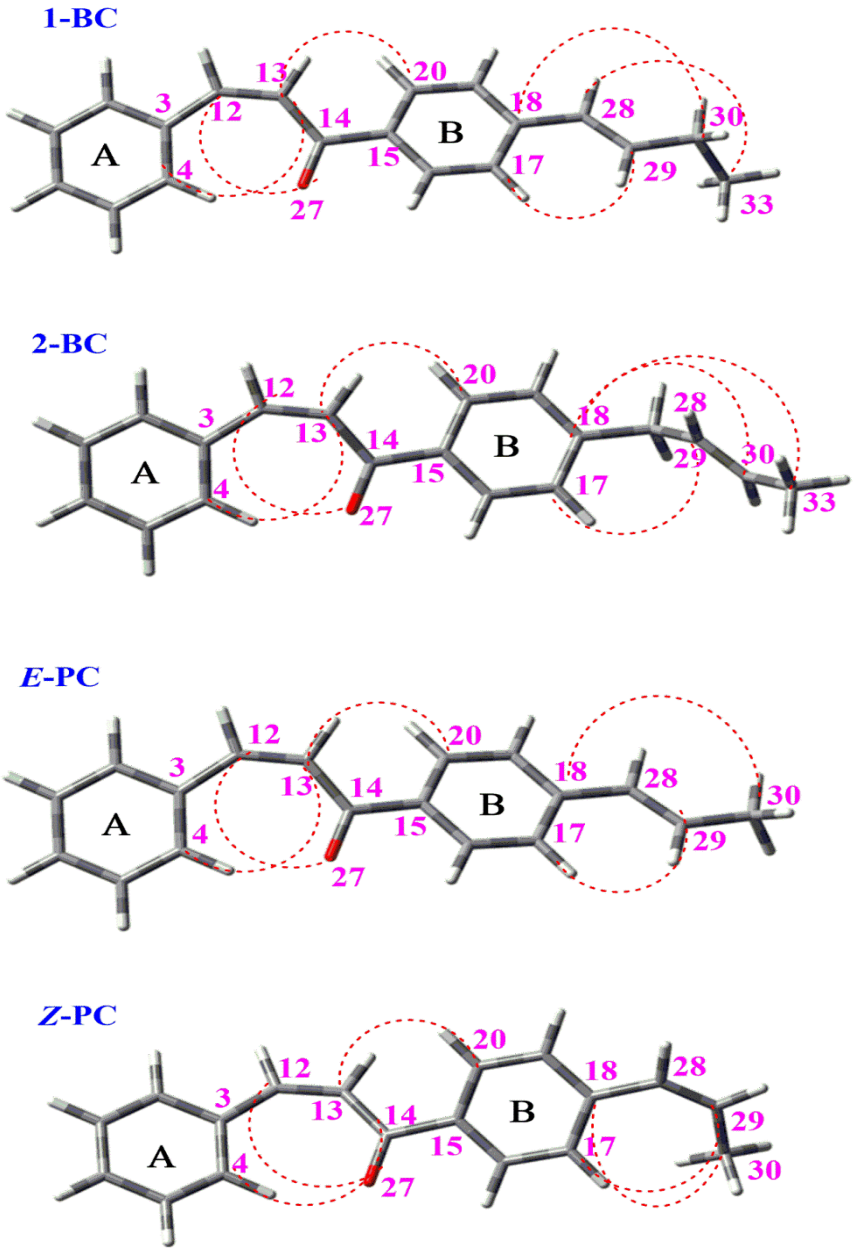

Scheme (2):- Schematic numbering patterns representing the main dihedral angles and aromatic rings A and B for *cis* conformers.

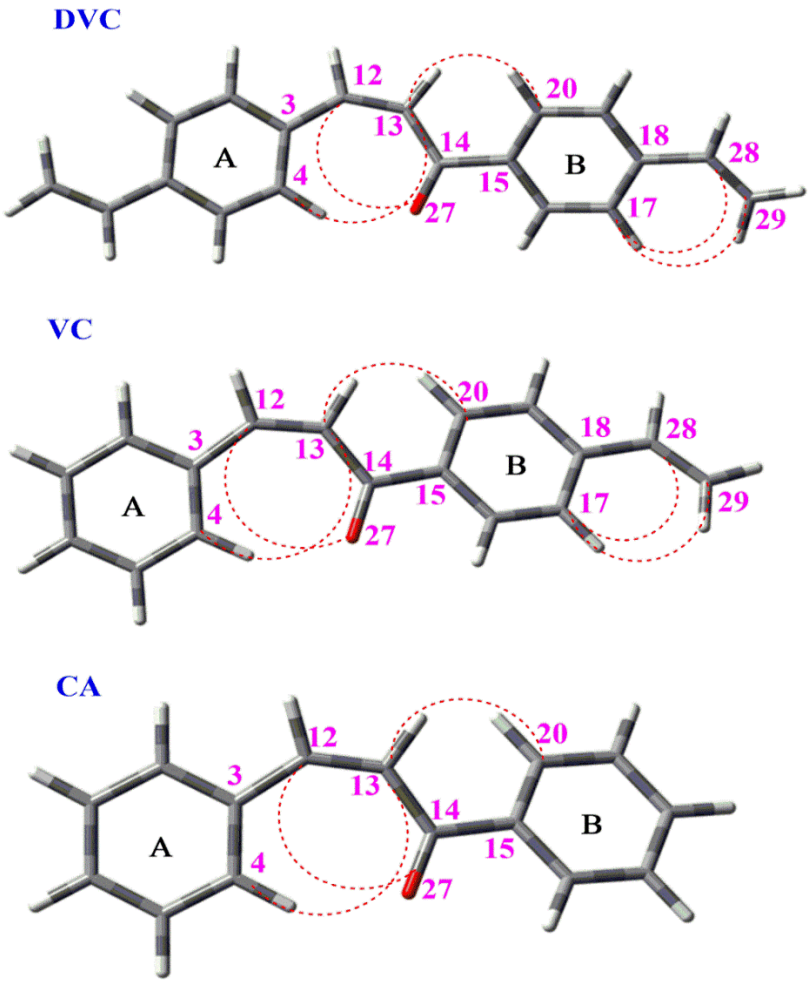

Scheme (3): -Schematic numbering patterns representing the main dihedral angles and aromatic rings A and B for *cis* DVC, VC and CA conformers.

The results obtained in table 3 illustrate the lower values of three angles of inclination (dihedral angles) in *cis* 1-BC conformer in the gas phase: C4-C3-C12-C13 (10.372°), C12-C13-C14-O27 (-18.791°), and C13-C14-C15-C20 (-19.437°) deviating by 1-3° from cis CA. Since the electron delocalization and inductive effects become more powerful and efficient as replacing 1-butenyl substituent with hydrogen in ring B (*cis* CA). Additionally, an intramolecular charge transfer is produced, which causes the stabilisation of the system [Kumar *et al.*, 2014]. As is highlighted in table 3, the planarity is increased in DVC, which lowers such dihedral angles values as: C4-C3-C12-C13, C12-C13-C14-O27, and C13-C14-C15-C20 by a deviation of 2-3° from *cis* CA. The coplanarity of two vinyl groups with the phenyl rings A and B enables conjugation, which further improves the □-electron delocalisation through the aromatic rings, carbonyl group, and olefins [Michelini *et al.*, 2018]. A slightly lower deviation is observed in the values of the three torsion angles upon substituting the chalcone moiety with one vinyl group, *Z*-propenyl, *E*-propenyl, and 2-butenyl groups. This is because the olefin groups and aromatic planes are coplanar, leading to a rise in the dihedral angles: VC (10.547°, -19.098°, -20.679°), *Z*-PC (-10.383°,18.902°,21.046°), *E*-PC (10.546°, -19.285°, -19.719°), and 2-BC (10.607°,-19.427°,-20.834°),respectively.

Therefore, it is evident that the order of planarity for the *cis* conformers becomes: DVC > 1-BC > *E*-PC > *Z*-PC > VC > 2-BC > CA. However, *E*-PC has lower coplanarity than *Z*-PC. This is rationalised as a result of the steric hindrance existing in the *Z*-PC conformer between the hydrogen atoms bonded to C3 methyl carbon and the carbon C17 at the meta-position of aromatic ring B. Due to the steric effect, a significant planarity deviation is seen in the torsion angle (C17-C18-C28-C29) compared with *E*-PC, which

is far closer to 0° and, therefore, more planar. Likewise, a subtle coplanarity deviation is evidenced on the torsion values on the C28-C29 bond axis of propenyl substituent. The torsion measured around this axis is closer to 180° in the *E*-PC conformer.

Table (3):- The torsion angles for studied conformers calculated by DFT(B3LYP) and 6-311++G(d,p).

		Cis			***Trans***		
	Dihedral angle(°)	Gas	n-Hexane	Ethanol	Gas	n-Hexane	Ethanol
1-BC	C4-C3-C12-C13	10.372	9.834	7.986	3.133	3.034	2.045
	C12-C13-C14-O27	-18.791	-19.440	-20.082	5.040	5.206	5.257
	C13-C14-C15-C20	-19.437	-19.821	-20.055	13.832	14.908	15.996
	C18-C28-C29-C30	179.872	179.902	179.939	179.676	179.710	179.752
	C28-C29-C30-C33	120.473	-120.616	-120.610	120.252	120.414	120.447
	C17-C18-C28-C29	-2.480	-2.548	-1.485	2.478	2.119	1.227
2-BC	C4-C3-C12-C13	10.607	9.918	5.579	1.700	1.261	1.253
	C12-C13-C14-O27	-19.427	-19.989	-19.553	4.435	4.490	5.396
	C13-C14-C15-C20	-20.834	-21.706	-22.842	14.170	16.098	16.728
	C18-C28-C29-C30	121.640	121.009	120.381	121.700	121.729	120.490
	C28-C29-C30-C33	179.639	179.726	179.718	179.529	179.660	179.757
	C17-C18-C28-C29	-61.235	-63.521	-75.146	59.945	67.923	73.658
E-PC	C4-C3-C12-C13	10.546	10.424	7.947	2.940	3.062	1.951
	C12-C13-C14-O27	-19.285	-20.813	-21.345	5.159	5.557	5.661
	C13-C14-C15-C20	-19.719	-19.877	-20.350	13.982	15.098	16.059
	C18-C28-C29-C30	179.964	179.932	-179.997	179.961	179.982	180.000
	C17-C18-C28-C29	-1.345	-0.225	-0.862	3.147	2.950	2.056
Z-PC	C4-C3-C12-C13	-10.383	-9.346	-6.272	2.584	2.321	0.806
	C12-C13-C14-O27	18.902	18.761	19.777	5.434	5.790	5.368
	C13-C14-C15-C20	21.046	21.725	22.144	15.166	16.026	16.993
	C18-C28-C29-C30	2.314	2.296	2.243	2.286	2.238	2.157
	C17-C18-C28-C29	35.065	34.066	32.310	34.536	33.705	32.245
DVC	C4-C3-C12-C13	-9.579	-9.068	-8.030	3.685	1.974	1.242
	C12-C13-C14-O27	17.320	17.231	17.447	5.340	4.321	3.922
	C13-C14-C15-C20	20.718	21.492	21.634	15.955	16.527	17.248
	C17-C18-C28-C29	1.692	1.222	0.614	4.639	4.473	3.678
	C18-C28-C29	127.360	127.288	127.139	127.283	127.206	127.071
VC	C4-C3-C12-C13	10.547	9.755	7.799	3.624	3.248	2.244
	C12-C13-C14-O27	-19.098	-19.606	-20.986	5.636	5.860	5.798
	C13-C14-C15-C20	-20.679	-21.187	-21.530	15.455	16.245	17.144
	C17-C18-C28-C29	-0.961	-0.275	0.198	3.324	3.650	3.167
	C18-C28-C29	127.353	127.284	127.104	127.296	127.219	127.079
CA	C4-C3-C12-C13	11.382	10.616	8.417	2.676	1.751	1.367
	C12-C13-C14-O27	-20.246	-20.161	-21.053	5.594	5.200	5.194
	C13-C14-C15-C20	-22.711	-23.393	-23.796	17.398	18.365	19.970

Moreover, the coplanarity of the conformers decreased with the solvent's polarity due to the enhancement in the intramolecular charge transfer interactions from the olefin portion to the chalcone moiety.

The planarity of the conformers was also significantly influenced by the geometry of the conformer. Table 3 illustrates that *trans* conformers generally have lower magnitudes of dihedral angles and are more planar since they lack the steric hindrance. This supports the intramolecular charge transfer, electron delocalisation, and π-conjugation that causes a higher dipole moment for *trans* conformers.

3.4 Thermodynamics

The heat of hydrogenation (*ΔH*) for the conformers was calculated:

H_2 + *Cis* chalcone → Hydrogenated *cis* alkenyl chalcone

The values of *ΔH* for H_2 molecule were taken as constants values (-1.166202 Hartree -gas phase, -1.166262 Hartree -n-hexane, and -1.166362 Hartree – ethanol).

Table 4 illustrates the values of ΔH in Hartree increase in the following trend: 1-BC > 2-BC > DVC > *E*-PC > *Z*-PC> VC > CA. Consequently, *ΔH* generally tends to increase as the molecules' stability decreases and decreases as the polarity of the solvent increases. Moreover, hydrogenated conformers are generally shown to have lower total electronic energies and enthalpies of hydrogenation in the gas phase and solvent media. Furthermore, *trans* conformers appeared to have lower magnitudes of *H* in both

hydrogenated and non-hydrogenated forms than their corresponding *cis* isomers. However, the enthalpy of hydrogenation was found to be much lower in *cis* conformers.

Table (4):- The non-hydrogenated and hydrogenated cis conformers with their heat of hydrogenation (H) in hartree units computed by DFT/B3LYP// (6-311++G(d,p) method. ΔH evaluated as result of subscription between hydrogenated and non-hydrogenated (H) conformers in Hartree.

	Phase	***H*** **(a.u)**	***H*** **(a.u)**	***ΔH*** **x10^{-2}** **(a.u)**
CA	Gas	-653.961493	-654.888300	73.47
	n-Hexane	-653.964168	-654.88599	23.43
	Ethanol	-653.969465	-654.816709	21.83
VC	Gas	-731.346542	-732.280933	23.11
	n-Hexane	-731.349515	-732.297507	21.83
	Ethanol	-731.365475	-732.327899	20.39
DVC	Gas	-808.732108	-809.713213	18.49
	n-Hexane	-808.735291	-809.756868	14.50
	Ethanol	-808.741665	-809.846552	6.22
E-PC	Gas	-770.647044	-771.621326	19.12
	n-Hexane	-770.650180	-771.630632	18.65
	Ethanol	-770.656308	-771.643746	17.85
Z-PC	Gas	-770.642488	-771.614486	19.44
	n-Hexane	-770.645405	-771.620598	19.12
	Ethanol	-770.651224	-771.632522	18.49
1-BC	Gas	-809.941385	-810.953065	15.46
	n-Hexane	-809.945347	-811.902823	-79.04
	Ethanol	-809.952086	-811.937990	-81.91
2-BC	Gas	-809.937035	-810.945040	15.78
	n-Hexane	-809.941873	-811.729604	-62.15
	Ethanol	-809.948276	-811.835654	-72.03

In this study, thermal energy (*TE*), entropy (*S*), and heat capacity at constant volume (C_v), were evaluated for the geometry-optimised *cis*-alkenyl-substituted conformers of chalcone at standard conditions. The results tabulated in tables 5 and 6 indicated that the decrease in the magnitudes of *TE*, *S*, and C_v obeys following pattern: 2-BC > 1-BC > DVC > *E*-PC > *Z*-PC > VC > CA. Consequently, it is suggested that the most stable conformer *cis* 2-BC constitutes largest *TE*, *S* and C_v, after that *cis* 1-BC and *cis* DVC come in the series, while the least stable conformers *cis* (VC and CA) possessed the lowest magnitudes. The results also show that the polarity influences the values of *TE*, *S*, and C_v. *S* and C_v grow up with the solvent's dielectric constant (ethanol > n-hexane>gas), whereas *TE* behaves conversely. Moreover, the conformers' geometry greatly affected the values of *TE*, *S*, and C_v. Studied *trans* conformers generally possess higher *TE*, *S*, and C_v than *cis* conformers due to their higher resonance stabilisation, which is associated with the better π-conjugation and electron delocalisation present. Additionally, unlike *cis* conformers, the values of *S* and C_v in *trans* conformers fall as in the following order: gas > n-hexane > ethanol.

Table (5): Entropy (S) and heat capacity (C_v) for the geometry optimized conformers at standard conditions computed in the gas phase, n-hexane and ethanol solvent at the B3LYP/6-311++G(d,p) level.

		S Cal/Mol-Kelvin			C_v Cal/Mol-Kelvin		
Conformers		Gas	Hexane	Ethanol	Gas	Hexane	Ethanol
CA	Electronic	0.000	0.000	0.000	0.000	0.000	0.000
	Translational	41.902	41.902	41.902	2.981	2.981	2.981
	Rotational	32.681	32.682	32.686	2.981	2.981	2.981
	Vibrational	42.856	43.122	43.796	44.625	44.630	44.641
	Total	117.439	117.706	118.384	50.586	50.592	50.602
VC	Electronic	0.000	0.000	0.000	0.000	0.000	0.000
	Translational	42.254	42.254	42.254	2.981	2.981	2.981
	Rotational	33.518	33.521	33.529	2.981	2.981	2.981
	Vibrational	55.244	55.766	56.067	53.549	53.564	53.570
	Total	131.015	131.541	131.850	59.511	59.525	59.532
DVC	Electronic	0.000	0.000	0.000	0.000	0.000	0.000
	Translational	42.568	42.568	42.568	2.981	2.981	2.981
	Rotational	34.325	34.323	34.325	2.981	2.981	2.981
	Vibrational	66.345	66.917	66.697	62.450	62.423	62.416
	Total	143.238	143.807	143.589	68.412	68.384	68.378
E-PC	Electronic	0.000	0.000	0.000	0.000	0.000	0.000
	Translational	42.427	42.427	42.427	2.981	2.981	2.981
	Rotational	33.988	34.000	34.002	2.981	2.981	2.981
	Vibrational	63.066	63.834	63.751	58.936	58.965	58.988
	Total	139.481	140.261	140.180	64.897	64.927	64.950
Z-PC	Electronic	0.000	0.000	0.000	0.000	0.000	0.000
	Translational	42.427	42.427	42.427	2.981	2.981	2.981
	Rotational	33.961	33.962	33.963	2.981	2.981	2.981
	Vibrational	61.170	61.237	62.183	58.619	58.629	58.669
	Total	137.558	137.625	138.573	64.581	64.591	64.631
2-BC	Electronic	0.000	0.000	0.000	0.000	0.000	0.000
	Translational	42.591	42.591	42.591	2.981	2.981	2.981
	Rotational	34.485	34.481	34.482	2.981	2.981	2.981
	Vibrational	70.642	56.986	50.828	63.755	59.875	58.036
	Total	147.718	134.057	127.901	69.717	65.836	63.998
1-BC	Electronic	0.000	0.000	0.000	0.000	0.000	0.000
	Translational	42.591	42.591	42.591	2.981	2.981	2.981
	Rotational	34.505	34.508	34.514	2.981	2.981	2.981
	Vibrational	68.759	61.859	54.634	63.699	61.734	59.693
	Total	145.855	138.957	131.739	69.661	67.696	65.655

Table (6): Thermal Energy (*TE*) in KCal/Mol for the *cis* geometry optimized conformers at standard conditions computed in the gas phase, n-hexane and ethanol solvent at the B3LYP/6-311++G(d,p) level.

		Gas	n-Hexane	Ethanol
CA	Electronic	0.000	0.000	0.000
	Translational	0.889	0.889	0.889
	Rotational	0.889	0.889	0.889
	Vibrational	147.118	147.110	147.091
	Total	148.895	148.887	148.868
VC	Electronic	0.000	0.000	0.000
	Translational	0.889	0.889	0.889
	Rotational	0.889	0.889	0.889
	Vibrational	169.138	169.112	169.081
	Total	170.916	170.889	170.859
DVC	Electronic	0.000	0.000	0.000
	Translational	0.889	0.889	0.889
	Rotational	0.889	0.889	0.889
	Vibrational	191.148	191.160	191.146
	Total	192.925	192.938	192.924
E-PC	Electronic	0.000	0.000	0.000
	Translational	0.889	0.889	0.889
	Rotational	0.889	0.889	0.889
	Vibrational	187.622	187.571	187.510
	Total	189.399	189.348	189.288
Z-PC	Electronic	0.000	0.000	0.000
	Translational	0.889	0.889	0.889
	Rotational	0.889	0.889	0.889
	Vibrational	187.768	187.744	187.680
	Total	189.546	189.522	189.457
2-BC	Electronic	0.000	0.000	0.000
	Translational	0.889	0.889	0.889
	Rotational	0.889	0.889	0.889
	Vibrational	206.168	204.962	204.623
	Total	207.946	206.740	206.400
1-BC	Electronic	0.000	0.000	0.000
	Translational	0.889	0.889	0.889
	Rotational	0.889	0.889	0.889
	Vibrational	206.357	205.755	205.297
	Total	208.134	207.532	207.074

3.5 C=O stretching vibration

The wavenumber of C=O stretching vibration typically appears within 1600 – 1700 cm^{-1} and is influenced by the inductive, conjugation, steric hindrance, and unshared pair of electrons on the oxygen atom [Panicker *et al.,* 2015]. The C=O stretching vibration has been calculated for the *cis* conformers, and the results are depicted in table 7. *Cis* 1-BC appeared to have the lowest energy and the most significant shifts (7 cm^{-1}-gas, 6 cm^{-1}-n-hexane, and 6 cm^{-1}-ethanol) in the magnitudes of vibrational frequencies, followed by *cis* DVC and *E*-PC. This is attributed to underestimating the large degree of π-electron delocalisation arising from the extended conjugation in these molecules. The least conjugated conformer *cis* VC caused a lower shift (3 cm^{-1}) due to the lower conjugation in this molecule.

The values of C=O stretching vibration are also influenced by the liquid's dielectric constant, as illustrated in table 7. A noticeably larger deviation (>30 cm^{-1}) in the C=O wavenumbers was observed in n-hexane as compared with the more polar solvent (ethanol). This deviation occurs due to a weaker hydrogen bonding interaction between C=O and n-hexane than between C=O and OH in ethanol solvent [Wang *et al.*, 2014; Kolling, 1999]. Furthermore, the infrared intensity of the band (I_{IR}) for C=O absorption appeared to depend on the conformer's structure and the polarity of the solvent. The *cis E*-PC conformer displayed the most intense bands for the C=O stretching vibrations in the gas phase (225), n-hexane (292), and ethanol (406) solvents. The absorption band's intensity also increased with the solvent's polarity due to the more significant change in the dipole moment.

Table (7): Scaled and unscaled asymmetric C=O stretching vibrational frequencies (Freq.) (ν_{as} CO) with infrared intensities (I_{IR}) for *trans* [(Hussein, 2023)] and *cis* alkenyl conformers of chalcones computed by DFT(B3LYP)/6-311++G(d,p) in the gas phase, n-hexane and ethanol solvents.

	Phase	ν_{as} CO				I_{IR}	
		Freq. (unscaled)		Freq. (scaled)			
		trans	*cis*	*trans*	*cis*	*tran*	*cis*
CA	Gas	1718	1706	1645	1634	149	162
	n-Hexane	1709	1698	1637	1669	204	219
	Ethanol	1597	1682	1569	1654	664	357
VC	Gas	1715	1702	1642	1631	186	199
	n-Hexane	1706	1694	1634	1665	257	265
	Ethanol	1690	1679	1661	1651	419	344
DVC	Gas	1713	1700	1641	1629	186	199
	n-Hexane	1703	1692	1631	1663	259	266
	Ethanol	1687	1678	1658	1649	433	228
E-PC	Gas	1714	1700	1642	1628	164	225
	n-Hexane	1706	1692	1634	1663	115	292
	Ethanol	1688	1677	1659	1648	453	406
Z-PC	Gas	1715	1703	1642	1631	183	189
	n-Hexane	1706	1695	1634	1666	244	214
	Ethanol	1691	1678	1662	1649	319	387
1-BC	Gas	1714	1699	1642	1627	184	166
	n-Hexane	1705	1692	1633	1663	220	291
	Ethanol	1600	1676	1572	1648	431	403
2-BC	Gas	1717	1704	1644	1632	172	185
	n-Hexane	1708	1696	1636	1667	229	243
	Ethanol	1691	1680	1662	1652	364	364

Furthermore, the position and intensity of the C=O band are also influenced by the geometry of the conformer. As the *trans* conformers are generally more stable than *cis* conformers, better stabilisation of C=O is achieved in nonpolar solvents (n-hexane) due to the free π-electron delocalisation and lack of steric hindrance between the C=O group and the aromatic ring, which leads to a higher conjugation and results in lower values of carbonyl stretching wavenumbers. Despite the effective conjugation in *trans* conformers, a lower intensity band is obtained in a nonpolar solvent (n-hexane), which could result from lower stabilisation of the C=O group in a nonpolar solvent. However, a better stabilisation of the C=O group occurs in the more polar solvent (ethanol), nearly doubling the intensity of the C=O absorption band. In addition, in *trans* conformers, the frequency of the C=O group is unexpectedly shifted to a higher frequency in the more polar solvent (ethanol) (table 7).

4.CONCLUSION

The structural analysis of the *cis* conformers indicated that the stability of *cis* chalcone is influenced by the planarity of the conformer, solvent polarity and geometry of the conformer. Results found that *cis* 1-BC and 2-BC possess the highest stability and significantly improves the stability of *cis* CA followed by *cis* DVC and *cis* *E*-PC. Also, *cis* 1-BC has apparently higher stability than *cis* 2-BC because of being more planar and lack of steric hindrance. Likewise, *cis* *E*-PC is appeared to have lower value of negative total energy than *cis* *Z*-PC and hence, more stable. In addition, the stability is also seen to be influenced by the polarity of the solvent and followed this trend (ethanol > n-hexane > gas). This is because a better enhancement of the electron delocalization and π-resonance is achieved in the more polar solvent ethanol due to its high dielectric constant. In the case of *cis* VC, the results of the solvent stabilization gap have displayed a very big shift in two trends of (ethanol to n-hexane) and (ethanol to gas) possibly attributing to the nature of the stabilization of this conformer in ethanol. Moreover, the geometry of the conformer also produced a pronounced impact on the stability, as the *trans* conformers were generally seemed to have higher stabilities because of being more planar than *cis* conformers.

A greatest shift in the magnitudes of vibrational frequencies is resulted by the most stable conformer *cis* 1-BC associated with the effective electron delocalization and π-conjugation present. Conversely, smallest shift (3 cm^{-1}) in the vibrational frequencies has been observed in *cis* CA conformer. Further large deviation (>30 cm^{-1}) in the C=O wavenumbers was noticed in the non-polar solvent (n-hexane) caused by a weak hydrogen bonding interaction between C=O and n-hexane.

REFERENCES

Carlo, D. G., Mascolo, N., Izzo, A.A., and Capasso, F. (1999). Flavonoids: old and new aspects of a class of natural therapeutic drugs. Life Sci..65(4):337–353.

Zaini, M. F., Arshad, S., Thanigaimani, K., Khalib, N. C., Zainuri, D.A., Abdullah, M. and Razak, I. A. (2019) New Halogenated Chalcones: Synthesis, Crystal Structure, Spectroscopic and Theoretical Analyses for Third-Order Nonlinear Optical Properties. J. Mol. Struct. 1195 (4): 606–619.

Kostanecki, S. and Tambor, J. (1899) Ueber Die Sechs Isomeren Monooxybenzalace tophenone (Monooxychalkone). Eur. J. Inorg. Chem. 32(2): 1921–1926.

Abbas, A., Gökce, H., Bahc¸eli, S. and Naseer, M. M. (2014), Spectroscopic (FT-IR, Raman, NMR and UV-Vis.) and Quantum Chemical Investigations of (E)-3-[4-(Pentyloxy)Phenyl]-1-Phenylprop-2-En-1-One. J. Mol. Struct. 1075 (5): 352–364.

Zaini, M. F., Razak, I. A. and Anis, M. Z. (2019) Crystal Structure, Hirshfeld Surface Analysis and DFT Studies of (E) -1- (4-Bromophenyl) -3- (3-Fluoro- Phenyl) Prop-2-En-1-One. Res. Commun. 75(1): 58–63.

Goto, Y., Hayashi, A., Kimura, Y. and Nakayama, M. (1991) Second Harmonic Generation and Crystal Growth of Substituted Thienyl Chalcone. J. Cryst. Growth 108(3-4): 688–698.

Broichhagen, J., Frank, J. A. and Trauner, D. (2015) A Roadmap to Success in Photopharmacology. Acc. Chem. Res. 48 (7): 1947–1960.

Venkata, B., Lokesh, S., Prasad, Y. R. and Shaik, A. B. (2017) Synthesis and Biological Activity of Novel 2,5-Dichloro-3-Acetylthiophene Chalcone Derivatives. Indian J. Pharm. Educ. Res. 51 (4):679–690.

Ibrahim, T. S., Moustafa, A. H., Almalki, A. J., Allam, R. M., Althagafi, A., Shadab, M. and Mohamed, M. F. A. (2021) Novel Chalcone / Aryl Carboximidamide Hybrids as Potent Anti-Inflammatory via Inhibition of Prostaglandin E2 and Inducible NO Synthase Activities: Design, Synthesis, Molecular Docking Studies and ADMET Prediction. J. Enzyme Inhib. Med. Chem. 36 (1):1067–1078.

Escrivani, O.D., Charlton, L.R., Caruso, B.M., Burle-Caldas, A. G., Borsodi, G. P. M., Zingali, B. R., Arruda-, N., Palmeira-Mello, V.M., de Jesus, B. J., Souza, T. M. A., Abrahim-Vieira, B., Freitag-Pohl, S., Pohl, E., Denny, W. P., Rossi-Bergmann, B. and Steel, G.P. (2021) Chalcones Identify CTXNPx as a Potential Antileishmanial Drug Target. PLoS Negl. Trop. Dis. 15 (11): 1–23.

Qin, H., Zhang, Z., Lekkala, R., Alsulami, H. and Rakesh, K. P. (2020) hemistry Chalcone Hybrids as Privileged Scaffolds in Antimalarial Drug Discovery: A Key Review. Eur. J. Med. Chem. 193 (1): 112215.

Lakshminarayanan, B., Kannappan, N.and Subburaju, T. (2020) Synthesis and Biological Evaluation of Novel Chalcones with Methanesulfonyl End as Potent Analgesic and Anti-Inflammatory Agents. Int. J. Pharmaceutical Sci. Res. Biosci. 11 (10): 4974–4981.

Okolo, E. N., Ugwu, D. I., Ezema, B. E., Ndefo, J. C., Eze, F. U., Ezema, C. G., Ezugwu, J. A. and Ujam, O. T. (2021) New Chalcone Derivatives as Potential Antimicrobial and Antioxidant Agent. Sci. Rep. 11(5): 21781.

Kahssay, W. S., Hailu, S. G. and Desta, T. K. (2021) Design, Synthesis, Characterization and in Vivo Antidiabetic Activity Evaluation of Some Chalcone Derivatives. Drug Des Devel Ther. 17(15): 3119–3129.

Reddy, R. M., Aidhen, S. I., Reddy, A. U., Reddy, B. G., Ingle, K. and Mukhopadhyay, S. (2019) Synthesis of 4-C-β-D-Glucosylated Isoliquiritigenin and Analogues for Aldose Reductase Inhibition Studies. Eur. J. Org. Chem.2019(24):3937–3948.

Bui, T. H., Nguyen, N. T., Dang, P. H., Nguyen, H. X., Thanh, M. and Nguyen, T. (2016) Design and Synthesis of Chalcone Derivatives as Potential Non-Purine Xanthine Oxidase Inhibitors. Springer-plus 5 (1): 1789.

Zhuang, C., Zhang, W., Sheng, C., Zhang, W., Xing, C. and Miao, Z. (2017) Chalcone: A Privileged Structure in Medicinal Chemistry. Chem. Rev.117(12):7762–7810.

Xie, Y., Wang, Z., Wang, D., Zhou, Y., Lei, Y., Gao, W., Liu, M., Huang, X. and Wu, H. (2021) Reversible Photochromic Properties of 4,5,6-Triaryl-4: H -Pyran Derivatives in a Solid State. Mater. Chem. Front. 5 (8): 3413–3421.

Hussein, H.A. and Fadhil, G. F. (2020) Theoretical Investigation of Para Amino-Dichloro Chalcone Isomers,Part I : A DFT Structure — Stability Study. J Phys Org Chem. 4: 1–15.

Wachter, N. M., Rani, N., Zolfaghari, A., Tarbox, H. and Mazumder, S. (2020) DFT Investigations of the Unusual Reactivity of 2-Pyridine carboxaldehyde in Base-Catalyzed Aldol

Reactions with Acetophenone. J. Phys. Org. Chem. 33 (5): 1–14.

Naresh, P., Pramodh, B., Naveen, S., Ganguly, S., Panda, J., Sunitha, K., Maniukiewicz, W. and Lokanath, N. K. (2021) Cis and Trans Isomers of 1-(5-Bromothiophen-2-Yl)-3-(10-Chloroanthracen-9-Yl) Prop-2-En-1-On e: Synthesis and Characterization. J. Mol. Struct. 1236: 130228.

Hussein, H. A. (2023) A DFT- study of structural-stability, Mulliken charges, MEP, FMO, and NLO properties of *trans* alkenyl- substituted-chalcones conformers, theoretical study. Structural Chemistry.

Frisch, M.J., Trucks, G.W., Schlegel, H.B., Scuseria, G.E., Robb, M.A., Cheeseman, J.R., Scalmani, G., Barone, V., Mennucci, B., Petersson, G.A., Nakatsuji, H., Caricato, M., Li, X., Hratchian, H.P., Izmaylov, A.F., Bloino, J., Zheng, G., Sonnenberg, J.L., Hada, M., Ehara, M., Toyota, K., Fukuda, R., Hasegawa, J., Ishida, M., Nakajima, T., Honda, Y., Kitao, O., Nakai, H., Vreven, T., Montgomery, J.A.J.E., Jr, Peralta, F., Ogliaro, M.B.J.J., Heyd, E., Brothers, K., Kudin, N., Staroverov, V., Keith, N.T., Kobayashi, R., Normand, J., Raghavachari, K., Rendell, A., Burant, J.C., Iyengar, S.S., Tomasi, J., Cossi, M., Rega, N., Millam, J.M., Klene, M., Knox, J.E., Cross, J.B., Bakken, V., Adamo, C., Jaramillo, J., Gomperts, R., Stratmann, R.E., Yazyev, O., Austin, A.J., Cammi, R., Pomelli, C., Ochterski, J.W., Martin, R.L., Morokuma, K., Zakrzewsk, V.G., Voth, G.A., Salvador, P., Dannenberg, J.J., Dapprich, S., Daniels, A.D., Farkas, Ö., Foresman, J.B., Ortiz, J.V., Cioslowski, J. and Fox, D.J. (2009) Gaussian 09, Revision D.01. Gaussian, Inc., Wallingford CT.

Dennington, R., Keith, T. and Millam, J. (2009) Gauss View, Version 5. Semichem Inc., Shawnee Mission.

Stephens, P.J., Devlin, F.J., Chabalowski, C.F. and Frisch, M.J. (1994) Ab initio calculation of vibrational absorption and circular dichroism spectra using density functional force fields. J Phys Chem 98(45):11623–11627.

Becke, D.A. (1993) Density-functional thermochemistry. III. The role of exact exchange. J Chem Phys 98:5648–5652.

Lee, C., Yang, W. andParr, R.G. (1988) Development of the colic-salvetti correlation-energy formula into a functional of the electron density. Phys Rev B 37:785–789.

Tomasi, J., Mennucci, B. and Cancès, E. (1999) The IEF Version of the PCM Solvation Method: An Overview of a New Method Addressed to Study Molecular Solutes at the QM Ab Initio Level. J. Mol. Struct. THEOCHEM 464(1–3): 211–226.

Tomasi, J., Mennucci, B. and Cammi, R. (2005) Quantum Mechanical Continuum Solvation Models. Chem. Rev. 105 (8): 2999–3093.

Mohbiya, D. R. and Sekar, N. (2018) Tuning 'Stokes Shift' and ICT Character by Varying the Donor Group in Imidazo[1,5 a]Pyridines: A Combined Optical, DFT, TD-DFT and NLO Approach. Chemistry Select 3(6): 1635–1644.

Balci, K. and Akyuz, S. (2008) A vibrational spectroscopic investigation on benzocaine molecule. Vib Spectrosc 48(2):215–228.

Sundaraganesan N, Ilakiamani S, Saleem H, Wojciechowski PM, Michalska D (2005) FT-raman and FT-IR spectra, vibrational assignments and density functional studies of 5-bromo-2-nitropyridine. Spectrochim Acta - Part A Mol Biomol Spectrosc 61(13–14):2995–3001. https://doi.org/10.1016/j.saa.2004.11.016

Valverde, C., Ribeiro, Í.N., Soares, J.V.B., Baseia, B. and Osório, F.A.P. (2019) Prediction of the linear and nonlinear optical properties of a schiff base derivatives via DFT. Adv Condens Matter Phys.

Sobhi, C., Nacereddine K.A., Djerourou, A., Ríos-Gutiérrez, M. and Domingo, L.R. (2017) A DFT study of the mechanism and selectivities of the [3 + 2] cycloaddition reaction between 3-(benzylidene eamino) oxindole and trans-β-nitrostyrene. J Phys Org Chem 30(6):1–9.

Miar, M., Shiroudi, A., Pourshamsian, K., Oliaey, A.R. and Hatamjafari, F. (2021) Theoretical investigations on the HOMO–LUMO gap and global reactivity descriptor studies, natural bond orbital, and nucleus-independent chemical shifts analyses of 3-pheny lben zo[d]thiazo le-2(3h)-imine and its para-substituted derivatives: solvent and subs. J Chem Res 45(1–2):147–158.

Kumar, A., Deval, V., Tandon, P., Gupta, A. and D'Silva, E.D. (2014) Experimental and theoretical (FT-IR, FT-Raman, UV-Vis, NMR) spectroscopic analysis and first order hyperpolarizability studies of non-linear optical material: (2E)-3-[4-(methylsulfanyl) phenyl]-1-(4-nitrophenyl) prop-2-en-1-one using density functional theory. Spectrochim Acta - Part A Mol Biomol Spectrosc 130:41–53.

Michelini, L. J., Castro, M. R. C., Custodio, J. M. F., Naves, L. F. N., Vaz, W. F., Lobón, G. S., Martins, F. T., Perez, C. N. and Napolitano, H. B. (2018) A Novel Potential Anticancer

(2014) Effects of hydrogen bond and solvent polarity on the C = O stretching of bis (2-thienyl) ketone in solution effects of hydrogen bond and solvent polarity on the C = O stretching of bis (2-thienyl) ketone in solution. 9(2012):12450.

Kolling, W. O. (1999) Effect of Hydrogen Bonding Solvents on the Infrared Absorption Band for the Fundamental Vibration of the Carbonyl Group in 1,1,3,3-Tetramethylurea. Transactions of the Kansas Academy of Science. 102 (1):53-56.

Chalcone: Synthesis, Crystal Structure and Cytotoxic Assay. J. Mol. Struct. 1168, 309–315.

Panicker, C. Y., Varghese, H. T., Nayak, P. S., Narayana, B., Sarojini, B. K., Fun, H. K., War, J. A., Srivastava, S. K. and Alsenoy, C. V. (2015) Infrared Spectrum, NBO, HOMO-LUMO, MEP and Molecular Docking Studies (2E)-3-(3-Nitrophenyl)-1-[4-Piperidin-1-Yl] Prop-2-En-1-One.Spectrochim. Acta - Part A Mol. Biomol. Spectrosc. 148: 18–28.

Wang, H., Wang, L., Shen, S., Zhang, W., Li, M., Du, L., Zheng, X., Lee, D., Wang, H. and Wang, L.

خاندنا شێوکێ ئه لیکترونی ، جێگری،سیرموداینامیک،له رینه وه تایبه تیێن سیز ئه لکینایل جێ گرتیێن جالکون بڕێکا دینستی فانکشنل سیوری

پوخته

د ڤێ ڤه کولینێدا شێوک و جێگریا شه ش مادێن سیز جالکونی هاته ئه نجامدان بکارئینانا ڕێکا دفت/ب۳لی پ /٦-۳۱۱++ج(د،پ) ل دوخی گاز وشلدا.ده ر ئه نجامان دانه دیارکرن کو سز ۱-بیوتنایل جالکون ژ هه میان جێگر تره و جێگریا سز جالکون زێده ت که تن ب ۹.۷۸ * ۱۰٤

ک کل/مول د ددووخێ گازیدا.و جێگری هه ر وه سان زێده بو دگه ل زێده بونا جمسداریێ مادێ شل.مادێن ترانز د ڤه کولنا به ری ڤێدا جێگر تر دیارکرن ژبه ر پانیا وان.و هه ر وه سان سیز ۱-بیوتینایل جالکون مه زنترین گورانکاری د بهایئن له‌رینا کاربونیل گروپ یا سز جالکون ئه نجامدا (۷ سم$^{-1}$ د گاز،٦ سم$^{-1}$ د نورمل هیکسان و ٦ سم$^{-1}$ د ایثانلدا) پشتی وی سز دافینایل جالکون دهیتن وپاشی سز ترانز پروپینایل جالکون.هه ر وه سان دیاربو کو سز۲-بیوتینل جالکون بلینترین بهایێن سیرمودینه میکی یێن هیزا گه رمی، ئینتروپی و هیت کاپاستی بخو دگریتن.ترانز جالکون بهایێن جدا یین سیرموداینه میکی بخو دگرت هه ر وه سان ڕێگین جیاواز بخو دگرت.

الدراسه ل تشخقص ال هیکل,استقراریه و الثیرموداینامیکیه و الاهتزازیه المعوضات ال الکینایل سیز جالکون ب استخدام ال دینستي فانکشنلل ثیوري

الخلاصة

في هذا البحث، تم تشخیص التحلیل الهیکلي والاستقراریة لستة هیئات من الجالکون(***cis*** **chalcone**) مقارنة مع هیئات (**trans**)باستخدام طریقة **DFT-B3LYP** ومجموعة الأساس **6-311++G(d,p)** وجدت النتائج التي تم الحصول علیها أن **(1-BC) 1-Butenyl cis Chalcone** یتمتع بأکبر قدر من الاستقراریة. یبدو أن قطبیة المذیب والبنیة الهندسیة للهیئة لهما تأثیر کبیر على استقرار الهیئات. بالإضافة إلى ذلك، تبین أن **cis 1-BC** یسبب أعظم ازاحة (7 سم$^{-1}$ غاز، 6 سم$^{-1}$ -ن-هکسان و6 سم$^{-1}$ -إیثانول) في مقدار الترددات الاهتزازیة لـ **cis CA** غیر المعوضة متبوعة بـ ***cis*** جالکون.(**cis divinyl chalcone (DVC)** و**(E-PC) *E*-propenyl chalcone**

لقد تبین أن 2-بیوتینیل جالکون (2-BC) یشکل أعلى قیم الطاقة الحراریة(T-E) ، والإنتروبیا (S) -والسعة الحراریة (C_v) .